HHS Public Access

Author manuscript

Mov Disord. Author manuscript; available in PMC 2017 November 01.

Published in final edited form as:

Mov Disord. 2016 November ; 31(11): 1676–1684. doi:10.1002/mds.26713.

Levodopa modulates small-world architecture of functional brain networks in Parkinson disease

Brian D. Berman, MD, MS[1,2], **Jason Smucny, MS**[3], **Korey P. Wylie, MD**[3], **Erika Shelton, BS**[1], **Eugene Kronberg, PhD**[3], **Maureen Leehey, MD**[1], and **Jason R. Tregellas, PhD**[3,4]

[1]Department of Neurology, University of Colorado Anschutz Medical Campus, Aurora, CO USA

[2]Neurology Section, Denver VA Medical Center, Denver, CO USA

[3]Department of Psychiatry, University of Colorado Anschutz Medical Campus, Aurora, CO USA

[4]Research Service, Denver VA Medical Center, Denver, CO USA

Abstract

Background—PD is associated with disrupted connectivity to a large number of distributed brain regions. How the disease alters the functional topological organization of the brain, however, remains poorly understood. Furthermore, how levodopa modulates network topology in PD is largely unknown.

Objectives—We used resting state functional MRI (rsfMRI) and graph theory to determine how small-world architecture is altered in PD and affected by levodopa administration.

Methods—Twenty-one PD patients and 20 controls underwent functional MRI scanning. PD patients were scanned off medication and one hour after 200mg levodopa. Imaging data were analyzed using 226 nodes comprising 10 intrinsic brain networks. Correlation matrices were generated for each subject and converted into cost thresholded, binarized adjacency matrices. Cost-integrated whole brain global and local efficiencies were compared across groups and tested for relationships with disease duration and severity.

Results—Data from two patients and four controls were excluded due to excess motion. Patients off medication showed no significant changes in global efficiency and overall local efficiency, but in a subnetwork analysis did show increased local efficiency in Executive (p=0.006), and Salience (p=0.018) networks. Levodopa significantly decreased local (p=0.039) efficiency in patients except within the Subcortical network where it significantly increased local efficiency (p=0.007).

Corresponding author: Brian D. Berman, M.D., M.S., Department of Neurology, University of Colorado Anschutz Medical Campus, 12631 E. 17th Avenue, Mail Stop B-185, Aurora, CO 80045, brian.berman@ucdenver.edu, Office: 303-724-2194; Fax: 303-724-2212.

Authors' Roles: B.D.B.: Project conception, design, organization, and execution; clinical assessments and scanning of subjects; analysis of imaging data, drafting and revision of manuscript.
J.S.: Project conception and design; analysis of imaging data; drafting and revision of manuscript.
K.P.W.: Project conception and design; analysis of imaging data; drafting and revision of manuscript.
E.S.: Project organization and execution; subject recruitment and scanning.
E.K.: Analysis of imaging data; revision of manuscript.
M.L.: Project conception; revision of manuscript.
J.R.T: Project conception and design; revision of manuscript.

Financial Disclosure: All authors report no relevant disclosures concerning the research related to this manuscript.

Conclusions—Levodopa modulates global and local efficiency measures of small-world topology in PD suggesting that degeneration of nigrostriatal neurons in PD may be associated with a large-scale network reorganization, and that levodopa tends to normalize the disrupted network topology in PD.

Keywords

Parkinson disease; resting state fMRI; graph theory; levodopa

Introduction

The pathological hallmark of Parkinson disease (PD) is the degeneration of nigrostriatal dopaminergic neurons, leading to a deficiency of dopamine in the striatum and the early motor features of the disease.[1] Neuroimaging studies suggest that striatal dopamine depletion leads to disturbances affecting a number of broadly distributed neural circuits (See[2–4] for reviews). How the functional organization on the more widespread whole brain level is altered by the disease, however, remains poorly understood. Furthermore, how dopaminergic therapy modulates disrupted network topology in PD is largely unknown.

Graph theory has been used extensively to study the organization of human brain networks.[5] The “small-world” model conceptualizes the brain as a distributed, integrated system that processes information both locally within dense specialized clusters of connections and globally through critical long-distance connections.[6] Large-scale neural networks in the small-world model are optimized for high global and high local efficiency, thereby minimizing the energy consumed and resources required for effective information processing and communication.[7, 8]

Using graph theory-based methods in combination with resting state functional MRI (rsfMRI) data, researchers have begun to understand the network disturbances in PD that underlie its symptoms.[9–11] Generally, these studies have reported that PD is associated with disruptions to their small-world topological organization, and that resting-state reorganization may be associated with symptom expression. Changes to global and local network efficiency may even be able to distinguish between PD motor subtypes.[12] Although these studies have revealed that functional neuronal topology in PD can be altered at both the global and local level, to our knowledge no published studies have evaluated how dopaminergic therapy affects these abnormalities.

The aim of the current study was to use rsfMRI and graph theory to examine disturbances in the functional topology of resting-state neural networks in PD before and after administration of dopamine. We hypothesized that local efficiency would be altered in PD patients and, given that an effect of dopamine depletion on both global and local efficiency has been reported in healthy subjects,[13] that dopamine replacement would exert a normalizing effect on efficiency measures in PD patients.

Methods

Participants

All patients met UK Brain Bank criteria for clinical diagnosis of idiopathic PD.[14] Inclusion criteria included an age between 50 and 80, Hoehn & Yahr (H&Y) stage of I–III (assessed in the *off* medication state), and on a stable dose of dopaminergic medication with a history of a beneficial motor response to the medication. Age- and gender-matched healthy controls were recruited from the local community. Participants were excluded if they had any contraindications to MRI, an untreated psychiatric condition, or cognitive impairment as evidenced by a Montreal Cognitive Assessment (MoCA) score <26.[15] Patients were excluded if they had undergone deep brain stimulation surgery, unpredictable motor fluctuations, dystonia, severe tremor, or dyskinesias to limit confounding of imaging data and motion effects. A total of 21 PD patients and 20 controls were enrolled in the study. Data from two PD patients and four healthy controls were excluded based on our motion criteria (see Supplementary Material) resulting in 19 patients and 16 controls being included in the final analysis (Table 1).

Standard protocol approvals, registrations, and patient consents

All participants gave written informed consent for the research protocol, which was approved by the Colorado Multiple Institutional Review Board.

Clinical Assessments

Motor symptoms in PD patients were evaluated both in a practically defined *off* state (>12 hours after last dopaminergic medication) and in an *on* state defined as one hour following 200mg of levodopa (two tablets of immediate release carbidopa/levodopa 25/100) at both a screening visit and at the time of MRI scanning. Motor severity was evaluated using Part III of the Movement Disorder Society-Unified Parkinson Disease Rating Scale (MDS-UPDRS).[16] A motor evaluation was performed at a screening visit in order to assess tolerability and response to levodopa, as well as provide an opportunity to exclude subjects if they had tremor, dystonia or dyskinesias that were felt may interfere with MRI scanning. Screening visits were performed within a minimum of three months before MRI scanning (mean±SD: 24.2±21.6 days). Overall symptom severity was evaluated using the total MDS-UPDRS score.

MRI Scanning

All participants underwent rsfMRI using a 3T GE Signa HDx system. A high-resolution, T1-weighted anatomical MRI was obtained for spatial normalization to standard Montreal Neurological Institute (MNI) space. Resting state fMRI data were acquired using gradient-echo echo planar imaging (EPI) sequences. Six-minute resting state scans were used to lessen possibility that subjects would fall asleep in the scanner and respiratory rate was actively monitored to further ensure subjects were not tending to fall asleep. After completing an initial rsfMRI scanning session in the *off* state, PD patients were given 200mg of levodopa and rescanned one hour afterward. See Supplementary Material for more details of the MRI scanning methods.

Anatomical Parcellation

Volumes were separated into 5mm radius regions-of-interest (ROIs) centered on MNI coordinates that comprise intrinsic brain networks defined by a recent meta-analytic study.[17] Coordinates classified as "unknown" in that study were not included in our study, resulting in ROIs being classified as Auditory Network (AUD), Cingulo-Opercular Network (CO), Dorsal Attention Network (DA), Default Mode Network (DMN), Executive Network (EXE), Salience Network (SAL), Sensorimotor Network (SOM), Subcortical Network (SUB), Ventral Attention Network (VA), or Visual Network (VIS).[17]

RsfMRI Pre-processing

Time series were calculated by taking the mean of the voxel time-series within each ROI. Possible spurious variance was removed from the data through linear regression. These were 1) six head motion parameters obtained during the spatial realignment step, 2) cerebrospinal fluid signal, 3) white matter signal, 4) global signal averaged over gray matter for the whole brain, and 5) simultaneous surface electromyography (EMG) acquired motion regressor (see below). Time series were linearly detrended and temporally band-pass filtered (0.01–0.1Hz). Images were normalized to a standard EPI template in MNI space, resampled to 3 mm isotropic voxels, and spatially smoothed using a Gaussian kernel of 6 mm full-width at half-maximum.

Motion Assessment and Correction

See Supplementary Material for details of steps taken to evaluate motion during rsfMRI scanning and account for motion artifact including spatial realignment, censoring of motion-confounded time points,[18] and simultaneous EMG monitoring. These steps led to the removal of all imaging data acquired on two patients and four controls, and the imaging data acquired on two patients in the *off* state and on two different patients in *on* state, from our analyses.

Correlation Matrix Construction

Correlation matrices for each subject were generated by calculating the absolute value of the correlation in BOLD signal over time between each pair of ROIs. The diagonal elements of each matrix were set to zero to assure compliance with Brain Connectivity Toolbox functions (see below). Mean correlation coefficients were used as a global measure of functional connectivity.

Graph Construction

We constructed graphs using each ROI covering the functional networks noted above resulting in a total of 226 nodes. Consistent with prior work,[19] correlation matrices were converted into thresholded, binarized matrices across a range of wiring costs from 0.09 (9%) to 0.5 (50%) in steps of 0.01 (1%) across all possible connections. This range was used because a cost of 0.09 is approximately the lowest cost of a fully connected network and 0.5 is a typical upper bound of cost in a small world regime.[20, 21] The lower bound of 0.09 helps ensure that brain networks have lower global efficiency and higher local efficiency compared to random networks with relatively the same distribution of degree of connectivity. Wiring

costs greater than 0.5 were not used because above this threshold brain networks become more random and less small-world,[22] and weaker network connections are likely to be non-neuronal and/or strongly influenced by noise.[23] In the binarization process, each element of each subject's connectivity matrix was set to either 0 or 1 based on its value relative to the other elements of the matrix. For example, for a graph thresholded at 0.5 wiring cost, the weakest 50% of connections were set to 0, and the remaining elements set to 1. We examined unweighted, binary adjacency matrices in order to investigate the underlying topological organization of each subject's functional network independent of changes to absolute connectivity.

Network Topology Measures

Standard network measures were calculated as described previously,[24] using functions from the Brain Connectivity Toolbox.[25] The network cost was defined as the fraction of edges in a network compared to a saturated network with the same number of nodes. Network efficiency was represented as the inverse of the harmonic mean of the minimum path length using previously described equations.[24] Global efficiency, which provides a measure of the efficiency of information transfer throughout the entire brain network, was defined as the network efficiency of the entire network. Local efficiency, which reflects the network's capacity for regional specialization, was defined as the averaged efficiencies of all brain sub-networks comprised of a node and its neighbors.

Statistical Analysis

Independent samples and paired samples t-tests were used to compare whole brain connectivity and cost-integrated global and local efficiency measures between PD patients and controls and between patients *on* and *off* medication, respectively. Similarly, independent samples and paired samples t-tests were used to evaluate group differences within intrinsic sub-networks were most responsible for driving overall network effect. As our sample of subjects may not be fully representative of a population, we tested the reliability of our significant group differences by applying a bootstrapping resampling methodology to allow for a better estimation of the null distribution of network measures. Bootstrapping was performed using 1,000 bootstrap samples. Significance was defined as $p \leq 0.05$ for both the straight comparison and comparison with bootstrapping, and a trend was defined if either the straight comparison or comparison with bootstrapping showed $p \leq 0.05$. All statistical analyses were performed with SPSS Statistics 23 (IBM Corporation, Armonk, NY).

Behavioral Correlations

Lastly, we investigated clinical relevance of graph theory measures in our PD cohort. Whole brain connectivity and integrated global and local efficiency metrics for each patient in the *off* state were tested with a Spearman's rank correlation coefficient to evaluate for any monotonic relationships with disease duration and total MDS-UPDRS score (*off* medication). In addition, we investigated whether levodopa-induced changes in connectivity or integrated global and local efficiency correlated with percent change in total MDS-UPDRS following administration of levodopa. As these correlative analyses were exploratory, we considered correlations with $p < 0.05$ as significant.

Results

Participants

There were no significant differences in age, gender, handedness and MoCA scores between PD patients and healthy controls (Table 1). PD patients had mild-to-moderate disease and showed improvement in their MDS-UPDRS III motor scores in the *on* versus *off* medication state. All of the PD patients were taking either levodopa or a dopamine agonist or both at the time of enrollment. Two patients were taking trihexyphenidyl and none of participants were taking acetylcholinesterase inhibitors.

Correlation Matrices

Figure 1 shows the correlation matrices for the controls and PD patients *off* and *on* medication. Overall, PD patients *off* medication showed a decrease in mean functional connectivity. Following administration of levodopa, mean functional connectivity increased and tended to normalize toward the control pattern. These network-wide changes were further supported by comparison of mean connectivity for the nodes constituting each the individual networks (Table 2). All networks showed reduced connectivity in PD patients *off* medication compared to controls, as well as increases in connectivity after taking levodopa. Significantly decreased connectivity between controls and patients *off* medication was seen in the AUD and VIS networks, and a trend toward decreased connectivity (p=0.050, $p_{bootstrap}$=0.059) was seen in the SOM network. An increase in mean connectivity across all nodes in the brain following levodopa nearly met our significance threshold, with the increase being driven by the AUD, SOM, and SUB networks. Although the changes did not reach our threshold for significance, increases were also seen in the CO, DA, DMN, and EXE networks. After levodopa, PD patients showed no significant differences in mean connectivity compared to controls.

Network Topology Measures

Group averages of global and local efficiencies were calculated for controls, PD patients *off* medication, and PD patients after levodopa administration across cost thresholds ranging from 0.09 to 0.5 and plotted alongside global and local efficiencies generated from simulated random and lattice networks across the same cost range (Figure 2). Global and local efficiencies for our control and patient population were intermediate between those for random and lattice networks across our small-world range of costs (0.09–0.5) supporting that the networks investigated have small world properties. In a whole-brain analysis, PD patients *off* medication showed no significant change in global efficiency (controls: 0.239±0.014, PD *off*: 0.240±0.012; p=0.748, $p_{bootstrap}$=0.749) or overall local efficiency (Table 3). Levodopa significantly decreased local efficiency in PD patients and induced a non-significant decrease in global efficiency in PD patients (PD *off*: 0.240±0.012, PD *on*: 0.231±0.017; p=0.071, $p_{bootstrap}$=0.081). No significant differences in global or local efficiency were found between controls and PD patients in the *on* medication state.

Comparison testing of local efficiency within each individual sub-network between PD patients and controls showed that patients in the *off* medication state have significantly increased local efficiency of their EXE and SAL networks, and a trend toward increased

local efficiency in their DMN network (p=0.067, $p_{bootstrap}$=0.039; Table 3). Among PD patients, levodopa led to a significant decrease of local efficiency in their DA network, as well as trend toward decreased local efficiency in their EXE network (p=0.048, $p_{bootstrap}$=0.062). Relative to controls, PD patients in the *on* medication state showed a significant decrease in local efficiency in their SOM network and a significant increase in local efficiency in their SUB network.

Behavioral correlations

No significant correlations were found between disease duration and whole brain connectivity or global and local efficiency measures. Given the ability of outliers to exert an over-represented influence on linear correlations, we removed an outlier (total MDS-UPDRS > 2 standard deviations from the mean) before correlation testing with disease severity. This outlier otherwise did not have outlying data in any other components of our analyses. Even after removal of our one outlier, no significant correlations were found between total MDS-UPDRS and global and local efficiency measures, however a significant positive correlation was seen between whole brain connectivity and the total MDS-UPDRS (r=0.81, p<0.001; see Supplementary Figure).

Discussion

In this study, we applied graph theory-based analyses to rsfMRI data in order to investigate abnormalities in functional brain network topology in PD and the impact of dopaminergic therapy. We show that levodopa significantly reduces local efficiency, and that the reduction in local efficiency is largely driven by decreases in the DA, EXE, and SOM networks. Levodopa may also reduce global efficiency, but we did not find a statistically significant effect. Cost-integrated global efficiency was not significantly different between controls and patients *off* or *on* dopaminergic medication, but cost-integrated whole brain local efficiency showed an increased efficiency in patients *off* medication that failed to reach our significance threshold though still helps support that levodopa exerts a normalizing effect on local efficiency. These findings together suggest that the neurodegenerative process in mild-to-moderate PD patients is associated with large-scale network reorganization at the local level, and that levodopa leads to a relatively over-connected state at the local brain processing level.

Consistent with a number of prior rsfMRI studies in PD,[2–4] we found that PD patients have overall reduced functional connectivity at baseline across brain networks. Although less well studied, levodopa has generally been reported to normalize altered functional connectivity in PD.[2, 3, 26, 27] Our results suggest that mild-to-moderately affected PD patients have reduced connectivity affecting all brain sub-networks in the *off* medication state and that levodopa imparts a restoring effect across these networks. This is consistent with known degeneration of dopaminergic neurons in PD that disrupt more widespread cognitive and limbic circuits in addition to motor circuits;[2, 4, 28] however, non-dopaminergic systems are also affected in PD and could contribute to our finding widespread disturbances in functional connectivity.[29–31]

There is increasing evidence from a variety of neuroimaging studies that human brain networks exhibit small-world properties including high global and local efficiency.[6, 7, 20]

Global efficiency can be used as a measure of the overall capacity for parallel information transfer and integrated processing. Aging has been reported to reduce global efficiency,[32] and Alzheimer's disease has also been associated with reduced global efficiency.[33–35] Although levodopa led to a nearly significant reduction in global efficiency in our PD population, cost-integrated whole brain global efficiency of the composite network did not differ between patients and controls. A similar lack of global efficiency change was recently reported in a separate study that involved a similar cohort of PD patients.[11] Nevertheless, this finding is somewhat surprising as the pharmacological blockade of dopamine neurotransmission in healthy adults has been reported to decrease global network efficiency.[20] In a magnetoencephalography (MEG) study, preserved global efficiency was observed in the early motor stage of PD.[36] Longitudinal analysis in a group of PD patients with longer disease duration, however, showed a progressive loss of functional global efficiency. Thus, a possible explanation for the lack of detectable changes in global efficiency in our PD patients may be that they had too mild of disease. Another possible explanation is that this study, in addition to the rsfMRI study by Skidmore et al,[9] used weighted networks, which may have led to results influenced by the presence of absolute overall reductions in connectivity. Our results were generated using unweighted, binary networks, which enabled us to examine network topology in PD independent of absolute connectivity.[37]

In our mild-to-moderately affected PD cohort, we found that levodopa induced significant reductions in cost-integrated local efficiency. Patients *off* medication also showed an increase in overall local efficiency and a levodopa-induced reduction in global efficiency, however these changes did not reach our threshold for significance. These findings suggest that the chronically depleted dopamine state of PD leads to a brain network reorganization that is a more clustered and lattice-like, possibly because lattice-like configurations are overall less costly.[38] Levodopa in this framework then decreases clustering and imparts a normalization effect on network organization. As the economic small-world model involves a balance between global and local efficiency,[7, 8, 39] the levodopa-induced reduction in integrated global efficiency could represent a compensatory response in order to maintain small-world topology.

By investigating local efficiency changes across the sub-networks defined in our parcellation step, we found increases in integrated local efficiency in PD patients *off* medication within the DMN, EXE and SAL networks. Levodopa tended to exert a normalizing effect on local efficiencies within the DMN, EXE and SAL networks, but it also led to a significant increase in local efficiency within the SUB network, and a significant decrease in local efficiency within the SOM network compared to controls. The DMN, EXE, and SAL networks are often referred to as the “core” neurocognitive networks critical to maintaining effective neural communication and their dysfunction has been established as playing a key role in the pathophysiology of a variety of neurological disorders.[40] Abnormal coupling between these core networks using rsfMRI has recently been reported in PD,[41] and is thought to stem from dysfunctional interactions between these networks and the striatum.[42, 43] As such, it is plausible that reduced striatal dopamine in PD specifically disturbs the functional integration within the core neurocognitive networks and that dopamine therapy is effective at normalizing their aberrant coupling. Since the SUB network

includes the basal ganglia and therefore contains a dense collection of dopamine receptors, the hyperstimulating effect of levodopa could stem from alterations in the density or sensitivity of postsynaptic dopamine receptors that may accompany the loss of nigrostriatal neurons in PD.[44]

Large-scale neural networks in the small-world model are optimized for high global and local efficiency, which minimizes the energy consumed and resources required for the effective information processing and communication.[7, 8] Thus, changes in the topological properties of brain networks could underlie clinical manifestations in PD. While we did not find a significant correlation between network topology measures and total MDS-UPDRS, we did find a positive correlation between whole brain connectivity and total MDS-UPDRS. In a similar study by Sule et al.,[11] a significant positive correlation was observed between the averaged local efficiency of the whole-brain network and total UPDRS scores. Although they used MEG to assess whole-brain functional network changes in PD, Olde Dubbelink et al. also reported that longitudinal changes in network topology were associated with worsening motor UPDRS scores and cognitive performance.[36] Since both of these studies used weighted correlation matrices to calculate network efficiency measures, their findings were dependent on changes in absolute connectivity. As such, it may be that underlying changes in functional connectivity more directly track overall disease severity. Further studies will be needed to help determine if changes in small-world network topology measures reflect clinically relevant phenomena and therefore hold promise as markers of disease severity.

One limitation of our study is the insufficient power to apply a strict correction for multiple comparisons. Given the relatively small sample size in our study, investigating changes to small-world architecture in greater numbers of patients is needed to help determine whether disruptions to brain network properties such as global and local efficiency play a key role in symptom expression in PD. Another potential limitation of our study is the use of a 6-minute rsfMRI scan length. Although longer scan times with PD patients could confound data by increasing the possibility that patients fall asleep, have greater movement, or experience a change in their *on* medication state during scanning, functional connectivity within resting state networks change on a very slow time scale and the use of a longer duration of acquisition could improve reliability of the data.[45] Furthermore, while all participants were visually monitored during rsfMRI scanning, involuntary movements by patients that were not captured by EMG monitoring could have been missed and contributed to our findings. Finally, while we do not suspect that there is substantial variability in oral levodopa absorption in our mild-to-moderately affected PD patients, our study is limited by the lack of measuring blood levels of levodopa and therefore an inability to directly account for any variability in absorption. Prior studies, however, suggest the absorption and elimination of levodopa does not differ between PD patients who have either stable or fluctuating responses to oral levodopa,[46] nor between PD patients across different H&Y disease stages.[47]

In conclusion, we show for the first time that levodopa alters the local efficiency and to a lesser extent the global efficiency measures of small-world topology in mild-to-moderate PD patients. By investigating whole brain network topology independent of changes in absolute connectivity, our findings suggest that the degeneration of nigrostriatal neurons is associated

with large-scale network reorganization of brain networks. Our findings further demonstrate that levodopa can influence whole-brain neurophysiological dynamics, and highlight that dopaminergic medication status must be carefully considered when mapping functional networks with rsfMRI. Future clinical and translational expansion of this work includes testing whether changes to small-world architecture of resting state functional networks can help discriminate PD from other parkinsonian disorders or be used to quantify the therapeutic effects of dopaminergic therapy in PD.

Supplementary Material

Refer to Web version on PubMed Central for supplementary material.

Acknowledgement

The authors would like to thank all patients and control subjects for their participation and Debra Singel for her assistance with scanning all of the study participants.

Study funding: This work was supported by NIH/NCATS Colorado CTSI Grant Number KL2 TR001080, the University of Colorado Department of Neurology, and the University of Colorado Center for NeuroScience.

Financial Disclosures (for the preceding 12 months): Dr. Berman has received research grant support from the NIH (NIH/NCATS Colorado CTSI Grant Number KL2 TR001080), the Dana Foundation, and the Benign Essential Blepharospasm Research Foundation, Inc. Mr. Smucny has received research support from a Ruth L. Kirschstein National Research Service Award (F31-MH102879-02). Dr. Leehey has received research grant support from the NIH (MH078041-06), the Colorado Department of Public Health and Environment, and UC WorldMeds, LLC. Dr. Tregellas has received research grant support from the NIH (MH-089095, DK-103691, MH-102224), the VA Clinical Science Research and Development Service (CX000459) and the Brain & Behavior Research Foundation. Dr. Wiley, Ms. Shelton, and Dr. Kronberg report have no financial disclosures.

References

1. Greffard S, Verny M, Bonnet AM, et al. Motor score of the unified Parkinson disease rating scale as a good predictor of Lewy body-associated neuronal loss in the substantia Nigra. Archives of Neurology. 2006; 63(4):584–588. [PubMed: 16606773]
2. Tessitore A, Giordano A, De Micco R, Russo A, Tedeschi G. Sensorimotor connectivity in Parkinson's disease: the role of functional neuroimaging. Frontiers in neurology. 2014; 5:180. [PubMed: 25309505]
3. Prodoehl J, Burciu RG, Vaillancourt DE. Resting state functional magnetic resonance imaging in Parkinson's disease. Curr Neurol Neurosci Rep. 2014; 14(6):448. [PubMed: 24744021]
4. Poston K, Eidelberg D. Functional brain networks and abnormal connectivity in the movement disorders. Neuroimage. 2012; 62(4):2261–2270. [PubMed: 22206967]
5. Reijneveld JC, Ponten SC, Berendse HW, Stam CJ. The application of graph theoretical analysis to complex networks in the brain. Clin Neurophysiol. 2007; 118(11):2317–2331. [PubMed: 17900977]
6. Stam CJ, van Straaten EC. The organization of physiological brain networks. Clin Neurophysiol. 2012; 123(6):1067–1087. [PubMed: 22356937]
7. Bullmore E, Sporns O. The economy of brain network organization. Nat Rev Neurosci. 2012; 13(5): 336–349. [PubMed: 22498897]
8. Latora V, Marchiori M. Efficient behavior of small-world networks. Physical review letters. 2001; 87(19):198701. [PubMed: 11690461]
9. Skidmore F, Korenkevych D, Liu Y, He G, Bullmore E, Pardalos PM. Connectivity brain networks based on wavelet correlation analysis in Parkinson fMRI data. Neurosci Lett. 2011; 499(1):47–51. [PubMed: 21624430]
10. Gottlich M, Munte TF, Heldmann M, Kasten M, Hagenah J, Kramer UM. Altered resting state brain networks in Parkinson's disease. PLoS One. 2013; 8(10):e77336. [PubMed: 24204812]

11. Tinaz S, Lauro P, Hallett M, Horovitz SG. Deficits in task-set maintenance and execution networks in Parkinson's disease. Brain Struct Funct. 2015
12. Zhang D, Liu X, Chen J, Liu B. Distinguishing patients with Parkinson's disease subtypes from normal controls based on functional network regional efficiencies. PLoS One. 2014; 9(12):e115131. [PubMed: 25531436]
13. Carbonell F, Nagano-Saito A, Leyton M, et al. Dopamine precursor depletion impairs structure and efficiency of resting state brain functional networks. Neuropharmacology. 2014; 84:90–100. [PubMed: 24412649]
14. Hughes AJ, Daniel SE, Kilford L, Lees AJ. Accuracy of clinical-diagnosis of idiopathic Parkinson's disease - A clinicopathological study of 100 cases. Journal of Neurology Neurosurgery and Psychiatry. 1992; 55(3):181–184.
15. Damian AM, Jacobson SA, Hentz JG, et al. The Montreal Cognitive Assessment and the Mini-Mental State Examination as Screening Instruments for Cognitive Impairment: Item Analyses and Threshold Scores. Dementia and Geriatric Cognitive Disorders. 2011; 31(2):126–131. [PubMed: 21282950]
16. Goetz CG, Tilley BC, Shaftman SR, et al. Movement Disorder Society-Sponsored Revision of the Unified Parkinson's Disease Rating Scale (MDS-UPDRS): Scale Presentation and Clinimetric Testing Results. Movement Disorders. 2008; 23(15):2129–2170. [PubMed: 19025984]
17. Power JD, Cohen AL, Nelson SM, et al. Functional network organization of the human brain. Neuron. 2011; 72(4):665–678. [PubMed: 22099467]
18. Power J, Barnes K, Snyder A, Schlaggar B, Petersen S. Spurious but systematic correlations in functional connectivity MRI networks arise from subject motion. Neuroimage. 2012; 59(3):2142–2154. [PubMed: 22019881]
19. Zhang T, Wang J, Yang Y, et al. Abnormal small-world architecture of top-down control networks in obsessive-compulsive disorder. Journal of psychiatry & neuroscience : JPN. 2011; 36(1):23–31. [PubMed: 20964957]
20. Achard S, Bullmore E. Efficiency and cost of economical brain functional networks. Plos Computational Biology. 2007; 3(2):174–183.
21. Bullmore ET, Bassett DS. Brain graphs: graphical models of the human brain connectome. Annu Rev Clin Psychol. 2011; 7:113–140. [PubMed: 21128784]
22. Humphries MD, Gurney K, Prescott TJ. The brainstem reticular formation is a small-world, not scale-free, network. Proc Biol Sci. 2006; 273(1585):503–511. [PubMed: 16615219]
23. Kaiser M, Hilgetag CC. Nonoptimal component placement, but short processing paths, due to long-distance projections in neural systems. PLoS Comput Biol. 2006; 2(7):e95. [PubMed: 16848638]
24. Wylie KP, Rojas DC, Tanabe J, Martin LF, Tregellas JR. Nicotine increases brain functional network efficiency. Neuroimage. 2012; 63(1):73–80. [PubMed: 22796985]
25. Rubinov M, Sporns O. Complex network measures of brain connectivity: uses and interpretations. Neuroimage. 2010; 52(3):1059–1069. [PubMed: 19819337]
26. Kelly C, de Zubicaray G, Di Martino A, et al. L-Dopa Modulates Functional Connectivity in Striatal Cognitive and Motor Networks: A Double-Blind Placebo-Controlled Study. J Neurosci. 2009; 29(22):7364–7378. [PubMed: 19494158]
27. Baik K, Cha J, Ham J, et al. Dopaminergic modulation of resting-state functional connectivity in de novo patients with Parkinson's disease. Hum Brain Mapp. 2014; 35(11):5431–5441. [PubMed: 24938993]
28. Poletti M, De Rosa A, Bonuccelli U. Affective symptoms and cognitive functions in Parkinson's disease. J Neurol Sci. 2012; 317(1–2):97–102. [PubMed: 22503136]
29. Gratwicke J, Jahanshahi M, Foltynie T. Parkinson's disease dementia: a neural networks perspective. Brain. 2015; 138(Pt 6):1454–1476. [PubMed: 25888551]
30. Wen MC, Ng SY, Heng HS, et al. Neural substrates of excessive daytime sleepiness in early drug naive Parkinson's disease: A resting state functional MRI study. Parkinsonism Relat Disord. 2016
31. Yoo K, Chung SJ, Kim HS, et al. Neural substrates of motor and non-motor symptoms in Parkinson's disease: a resting FMRI study. PLoS One. 2015; 10(4):e0125455. [PubMed: 25909812]

32. Bullmore E, Fadili J, Maxim V, et al. Wavelets and functional magnetic resonance imaging of the human brain. Neuroimage. 2004; 23(Suppl 1):S234–249. [PubMed: 15501094]
33. Yao Z, Zhang Y, Lin L, et al. Abnormal cortical networks in mild cognitive impairment and Alzheimer's disease. PLoS Comput Biol. 2010; 6(11):e1001006. [PubMed: 21124954]
34. Stam CJ, Jones BF, Nolte G, Breakspear M, Scheltens P. Small-world networks and functional connectivity in Alzheimer's disease. Cereb Cortex. 2007; 17(1):92–99. [PubMed: 16452642]
35. He Y, Chen Z, Evans A. Structural insights into aberrant topological patterns of large-scale cortical networks in Alzheimer's disease. J Neurosci. 2008; 28(18):4756–4766. [PubMed: 18448652]
36. Olde Dubbelink KT, Hillebrand A, Stoffers D, et al. Disrupted brain network topology in Parkinson's disease: a longitudinal magnetoencephalography study. Brain. 2014; 137(Pt 1):197–207. [PubMed: 24271324]
37. Ginestet CE, Nichols TE, Bullmore ET, Simmons A. Brain network analysis: separating cost from topology using cost-integration. PLoS One. 2011; 6(7):e21570. [PubMed: 21829437]
38. Kitzbichler MG, Henson RN, Smith ML, Nathan PJ, Bullmore ET. Cognitive effort drives workspace configuration of human brain functional networks. J Neurosci. 2011; 31(22):8259–8270. [PubMed: 21632947]
39. Watts DJ, Strogatz SH. Collective dynamics of 'small-world' networks. Nature. 1998; 393(6684): 440–442. [PubMed: 9623998]
40. Menon V. Large-scale brain networks and psychopathology: a unifying triple network model. Trends Cogn Sci. 2011; 15(10):483–506. [PubMed: 21908230]
41. Putcha D, Ross RS, Cronin-Golomb A, Janes AC, Stern CE. Altered intrinsic functional coupling between core neurocognitive networks in Parkinson's disease. Neuroimage Clin. 2015; 7:449–455. [PubMed: 25685711]
42. Di X, Biswal BB. Modulatory interactions between the default mode network and task positive networks in resting-state. PeerJ. 2014; 2:e367. [PubMed: 24860698]
43. Alexander GE, Crutcher MD. Functional architecture of basal ganglia circuits: neural substrates of parallel processing. Trends Neurosci. 1990; 13(7):266–271. [PubMed: 1695401]
44. Hisahara S, Shimohama S. Dopamine receptors and Parkinson's disease. Int J Med Chem. 2011; 2011:403039. [PubMed: 25954517]
45. Birn RM, Molloy EK, Patriat R, et al. The effect of scan length on the reliability of resting-state fMRI connectivity estimates. Neuroimage. 2013; 83:550–558. [PubMed: 23747458]
46. Contin M, Riva R, Martinelli P, Cortelli P, Albani F, Baruzzi A. Pharmacodynamic modeling of oral levodopa: clinical application in Parkinson's disease. Neurology. 1993; 43(2):367–371. [PubMed: 8437704]
47. Contin M, Riva R, Martinelli P, Albani F, Avoni P, Baruzzi A. Levodopa therapy monitoring in patients with Parkinson disease: a kinetic-dynamic approach. Ther Drug Monit. 2001; 23(6):621–629. [PubMed: 11802094]

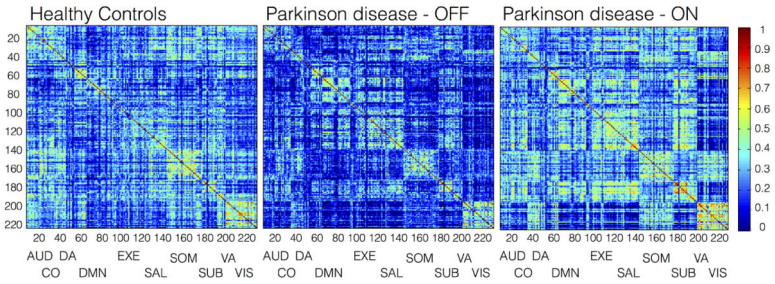

Figure 1.

Group-based correlation matrices for healthy controls and PD patients in the off and on medication state (one hour following levodopa administration). Networks evaluated include Auditory (AUD, 1–13), Cingulo-Opercular (CO, 14–27), Dorsal Attention (DA, 28–38), Default Mode (DMN, 39–95), Executive (EXE, 96–120), Salience (SAL, 121–138), Sensorimotor (SOM, 139–173), Subcortical (SUB, 174–186), Ventral Attention (VA, 187–195), and Visual (VIS, 196–226).

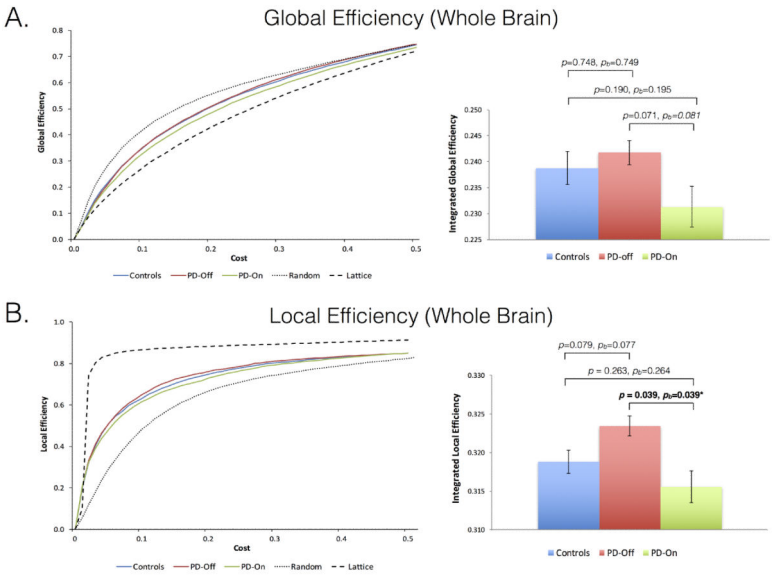

Figure 2.

Local (A) and global (B) efficiencies plotted as group average as a function of wiring cost (along with a random permutation network for visualization purposes) and as box plots of integrated efficiencies for each cohort and condition. Group comparisons performed using two-tailed t tests (two sample and paired), and tested for reliability using a boostrap (b) sampling. *Significant difference of $p \leq 0.05$.

Table 1

Subject demographic data

	PD patients N = 19	Healthy controls N = 16	*p*-value
Age, y	61.7 ± 7.8	61.3 ± 8.9	0.88
Gender (M:F)	11:8	9:8	0.65
Handedness (L:R)	2:17	2:14	0.86
MoCA	27.8 ± 1.5	28.2 ± 1.8	0.48
Disease stages, H&Y	2.18 ± 0.73	-	-
Disease duration, y	5.73 ± 3.45	-	-
LEDD, mg	546.8 ± 361.0	-	-
# taking levodopa	13 (68%)	-	-
# taking DA agonist	15 (79%)	-	-
# taking MAO-B	8 (42%)	-	-
# taking amantadine	2 (11%)	-	-
Initial side affected (L:R)	8:11	-	-
MDS-UPDRS (Total)			
Off	52.4 ± 15.5	-	-
On	43.3 ± 15.9		< 0.000
MDS-UPDRS I	9.4 ± 4.5	-	-
MDS-UPDRS II	9.5 ± 6.9	-	-
MDS-UPDRS III			
Off (MRI)	31.52 ± 9.8	-	-
On (MRI)	22.4 ± 9.2	-	< 0.000
MDS-UPDRS IV	2.0 ± 2.2	-	-
BDI	8.2 ± 5.8	-	-
NPI-Severity	2.1 ± 2.1	-	-

Values shown as mean ± sd except where indicated. P values calculated using two-tailed t tests except for gender differences tested using chi-square test. Abbreviations: BDI = Beck Depression Inventory; DA = dopamine; H&Y = Hoehn & Yahr score; LEDD = Levodopa equivalent daily dose; MDS-UPDRS = Movement Disorder Society-Sponsored Revision of the Unified Parkinson's Disease Rating Scale; MAO-B = monoamine oxidase B inhibitor; MoCA = Montreal Cognitive Assessment; NPI = Neuropsychiatric Inventory; PIGD = Postural Instability Gait Difficulty; TD = Tremor Dominant.

Table 2

Mean functional connectivity of networks across study cohorts.

NETWORK	Healthy Controls (HC)	Parkinson disease (PD) patients		T test comparisons (*p* value)[a/b]		
		Off	*On*	HC vs PD-Off	PD-Off vs PD-On	HC vs PD-On
Whole brain	0.27 ± 0.17	0.18 ± 0.12	0.29 ± 0.22	0.089/0.100	0.039/0.051	0.813/0.823
AUD	0.29 ± 0.19	0.17 ± 0.11	0.30 ± 0.24	0.028/0.040 *	0.013/0.007 *	0.936/0.934
CO	0.29 ± 0.18	0.19 ± 0.13	0.29 ± 0.24	0.089/0.112	0.043/0.062	0.916/0.925
DA	0.30 ± 0.18	0.20 ± 0.14	0.30 ± 0.23	0.105/0.104	0.057/0.057	0.950/0.960
DMN	0.23 ± 0.17	0.17 ± 0.13	0.28 ± 0.24	0.272/0.291	0.055/0.067	0.522/0.543
EXE	0.25 ± 0.20	0.18 ± 0.13	0.30 ± 0.25	0.259/0.276	0.063/0.082	0.531/0.536
SAL	0.27 ± 0.19	0.21 ± 0.14	0.29 ± 0.24	0.307/0.331	0.120/0.141	0.749/0.771
SOM	0.30 ± 0.17	0.19 ± 0.14	0.30 ± 0.23	0.050/0.059	0.021/0.025 *	0.997/0.994
SUB	0.26 ± 0.20	0.19 ± 0.16	0.32 ± 0.26	0.290/0.308	0.045/0.053	0.467/0.480
VA	0.29 ± 0.20	0.21 ± 0.14	0.29 ± 0.27	0.204/0.266	0.198/0.230	0.993/0.993
VIS	0.30 ± 0.18	0.16 ± 0.11	0.25 ± 0.20	0.007/0.010 *	0.120/0.121	0.424/0.430

Values under participant headings are mean ± s.d. of correlation coefficients measured across nodes constituting each intrinsic brain network. Network abbreviations: AUD = Auditory; CO = Cingulo-Opercular; DA = Dorsal Attention; DFM = Default Mode; EXE = Executive; SAL = Salience; SOM = Sensorimotor; SUB = Subcortical; VA = Ventral Attention; VIS = Visual. Comparison tested with two-tailed independent and paired t-tests,[a] and checked for reliability using bootstrap resampling with 1,000 samples.[b]

*Significant difference of $p \leq 0.05$.

Table 3

Integrated local efficiency for intrinsic networks across study cohorts.

NETWORK	Healthy Controls (HC)	Parkinson disease (PD) patients		T test comparisons (*p* value)[a/b]		
		Off	*On*	HCvs PD-Off	PD-Off vs PD-On	HCvs PD-On
Whole brain	0.319 ± 0.007	0.323 ± 0.006	0.316 ± 0.009	0.079/0.077	0.039/0.039 *	0.263/0.264
AUD	0.326 ± 0.016	0.317 ± 0.023	0.312 ± 0.031	0.231/0.231	0.662/0.667	0.125/0.147
CO	0.320 ± 0.019	0.323 ± 0.018	0.308 ± 0.021	0.670/0.678	0.184/0.197	0.118/0.119
DA	0.320 ± 0.017	0.324 ± 0.019	0.303 ± 0.013	0.575/0.555	0.011/0.016 *	0.052/0.058
DMN	0.310 ± 0.021	0.320 ± 0.011	0.317 ± 0.009	0.067/0.039	0.287/0.306	0.231/0.262
EXE	0.317 ± 0.014	0.329 ± 0.010	0.318 ± 0.019	0.006/0.007 *	0.048/0.062	0.831/0.844
SAL	0.313 ± 0.017	0.326 ± 0.013	0.321 ± 0.017	0.018/0.019 *	0.439/0.469	0.204/0.217
SOM	0.327 ± 0.011	0.327 ± 0.009	0.318 ± 0.015	0.909/0.914	0.087/0.097	0.039/0.041 *
SUB	0.315 ± 0.017	0.324 ± 0.014	0.335 ± 0.021	0.100/0.114	0.199/0.205	0.007/0.008 *
VA	0.321 ± 0.013	0.317 ± 0.019	0.321 ± 0.031	0.451/0.416	0.393/0.395	0.994/0.995
VIS	0.327 ± 0.011	0.319 ± 0.017	0.306 ± 0.044	0.098/0.105	0.289/0.285	0.064/0.108

Values under participant headings are mean ± s.d. of integrated local efficiency measured across nodes constituting each intrinsic brain network. Network abbreviations: AUD = Auditory; CO = Cingulo-Opercular; DA = Dorsal Attention; DMN = Default Mode; EXE = Executive; SAL = Salience; SOM = Sensorimotor; SUB = Subcortical; VA = Ventral Attention; VIS = Visual. Comparison tested with two-tailed independent and paired t-tests,[a] and checked for reliability using bootstrap resampling with 1,000 samples.[b]

*Significance difference of $p \leq 0.05$.